FEBS Letters 589 (2015) 3098–3106

FEBS Letters

journal homepage: www.FEBSLetters.org

Biochemical identification of the catalytic residues of a glycoside hydrolase family 120 β-xylosidase, involved in xylooligosaccharide metabolisation by gut bacteria

Davide A. Cecchini, Régis Fauré, Elisabeth Laville, Gabrielle Potocki-Veronese *

Université de Toulouse, INSA, UPS, INP, LISBP, 135 Avenue de Rangueil, F-31077 Toulouse, France
INRA, UMR792, Ingénierie des Systèmes Biologiques et des Procédés, F-31400 Toulouse, France
CNRS, UMR5504, F-31400 Toulouse, France

ARTICLE INFO

Article history:
Received 11 May 2015
Revised 4 August 2015
Accepted 6 August 2015
Available online 20 August 2015

Edited by Miguel De la Rosa

Keywords:
β-Xylosidase
Glycoside hydrolase family 120
Site-directed mutagenesis
Catalytic residue
Retaining mechanism
Bifidobacterium adolescentis

ABSTRACT

The β-xylosidase B from *Bifidobacterium adolescentis* ATCC15703 belongs to the newly characterized family 120 of glycoside hydrolases. In order to investigate its catalytic mechanism, an extensive kinetic study of the wild-type enzyme and mutants targeting the three highly conserved residues Asp^{393}, Glu^{416} and Glu^{364} was performed. NMR analysis of the xyloside hydrolysis products, the change of the reaction rate-limiting step for the Glu^{416} mutants, the pH dependency of E416A activity and its chemical rescue allowed to demonstrate that this GH120 enzyme uses a retaining mechanism of glycoside hydrolysis, Glu^{416} playing the role of acid/base catalyst and Asp^{393} that of nucleophile.

1. Introduction

In the last few years an increasing number of studies highlighted the deep interactions that exist between the human body, its gut microbiota, and dietary fibers. Only to cite few examples, the gut microbiota has been shown to be involved in the stimulation of the immune system, in providing resistance to pathogens and to be associated with human diseases such obesity [1], in type-2 diabetes [2,3] or atherosclerosis [4]. Thus, the modulation of the composition and/or activity of the intestinal microbiota by the administration of functional foods arouse an increasing interest to positively impact human health and digestive comfort. Functional foods are either probiotics (healthy bacteria), prebiotics (oligo- or polysaccharides compounds not digested by human enzymes), or symbiotics (mixtures of probiotics and prebiotics), which are able to specifically stimulate beneficial microorganisms, like bifidobacteria [5]. Together with fructooligosaccharides and transgalactooligosaccharides, xylooligosaccharides (XOS) are ones of the most studied prebiotics. Made up by D-xylopyranosyl (D-Xyl*p*) residues linked by β-(1,4) glycosidic linkages, and obtained from the degradation of xylan, an hemicellulose compound of fruits and vegetables, XOS consumption has been shown to stimulate bifidobacteria growth and to decrease cecal and fecal pH [6,7]. XOS also have immunomodulatory activity [8,9], inhibitory effect on precancerous colon lesions [6] and inhibitory effects on the growth of sulphite-reducing clostridia [10], whose metabolic end product, hydrogen sulfide, is a cytotoxic compound that could be implicated in inflammatory bowel diseases [11–14]. However little is known about the species and enzymes involved in their degradation. One of the major reason for this is the difficulty in isolating XOS degrading bacteria species,

Abbreviations: 3,4-dNP, 3,4-dinitrophenol; 3,4-dNP-β-D-Xyl*p*, 3,4-dinitrophenyl-β-D-xylopyranoside; GH, glycoside hydrolase; LG, leaving group; 4-MU, 4-methylumbelliferone; 4-MU-β-D-Xyl*p*, 4-methylumbelliferylβ-D-xylopyranoside; 2-NP, 2-nitrophenol; 2-NP-β-D-Xyl*p*, 2-nitrophenyl β-D-xylopyranoside; 4-NP, 4-nitrophenol; 4-NP-β-D-Xyl*p*, 4-nitrophenyl β-D-xylopyranoside; N_3-β-D-Xyl*p*, β-D-xylosyl azide; XOS, xylooligosaccharides; D-Xyl*p*, D-xylopyranosyl; *Ba*XylB, β-xylosidase B from *Bifidobacterium adolescentis* ATCC15703; TS, transition state; *Ts*XylC, β-xylosidase C from *Thermoanaerobacterium saccharolyticum* JW/SL-YS485

Author contributions: DAC and GPV conceived and supervised the study; DAC, RF and GPV designed experiments; DAC and RF performed experiments; DAC, RF, EL and GPV analyzed data; DAC, RF and GPV wrote the manuscript.

* Corresponding author at: Université de Toulouse, INSA, UPS, INP, LISBP, 135 Avenue de Rangueil, F-31077 Toulouse, France. Fax: +33 5 61 55 94 00.
E-mail address: veronese@insa-toulouse.fr (G. Potocki-Veronese).

http://dx.doi.org/10.1016/j.febslet.2015.08.012
0014-5793/

mainly because they live in a very complex ecosystem composed of 70% uncultivated bacteria, and because they establish complex trophic interactions with other microorganisms, that are difficult to reproduce in vitro. To address this issue, and circumvent the difficulty of bacterial cultivation, activity based functional metagenomics was previously used to target any possible Carbohydrate Active enZymes (CAZymes) [15] involved in the degradation of all commercialized prebiotics, including XOS, by ileal and colonic bacteria [16]. Among them was identified an enzyme classified in the glycoside hydrolase (GH) family GH120 of the CAZy classification (www.cazy.org) [15], taxonomically assigned to an uncultivated *Bifidobacterium adolescentis* species. This GH120 sequence was retrieved in the metagenome of numerous European and American subjects, indicating that this enzyme and its nearest homologs probably play a key role in the metabolization of XOS, derived either from prebiotics or from the hemicellulosic part of dietary fibers. Even truncated from the N-terminal residues in the metagenomic DNA insert, this sequence presents 98% protein sequence identity with that of *Ba*XylB, a β-xylosidase B (EC 3.2.1.37) from *B. adolescentis* ATCC15703, which is highly specific for short XOS (i.e. polymerisation degree range 3–6) [17]. GH120 *Ba*XylB associated with GH43 *Ba*XylC and GH8 *Ba*RexA are part of the *B. adolescentis* enzymatic toolbox with different but complementary substrate specificities to completely hydrolyse XOS [17,18]. The bacterium *Thermoanaerobacterium saccharolyticum* JW/SL-YS485 also exhibits such as arsenal including three β-xylosidases, non-classified *Ts*XylA, GH30 *Ts*XylB and GH120 *Ts*XylC. Today, the novel GH120 family gathers 67 sequences, all from bacteria. *Ba*XylB and *Ts*XylC are the sole GH120 enzymes that have been functionally characterized [17,19]. In addition, the crystallographic structure of *Ts*XylC, solved in 2012, constitutes the sole structural data for GH120 enzymes [20]. *Ts*XylC comprises two domains: the core domain that folds into a right-handed parallel β-helix and a small flanking region that folds into a β-sandwich domain. Both are involved in the active site formation and provide interactions for substrate binding. From the inspection of *Ts*XylC structures in complex with xylobiose and D-xylose, three carboxylic residues were identified in the active site. Since they are located near the anomeric *C*-1 carbon of the non-reducing D-xylosyl unit or close to the glycosidic oxygen, and because their mutation into alanine abolished the activity in preliminary assays using 4-nitrophenyl β-D-xylopyranoside (4-NP-β-D-Xyl*p*) as substrate, Asp^{382} and Glu^{405} were suggested as candidates for nucleophile and general acid/base catalytic residues respectively, while Glu^{353} would be involved in substrate binding. However, no further evidences were presented in this pioneer work to support this assumption. *Ts*XylC Asp^{382} and Glu^{405} thus appear as inferred catalytic residues in the CAZY database.

In the present work, the equivalent essential catalytic residues of *Ba*XylB were identified and their role in catalysis was confirmed by site-directed mutagenesis, detailed kinetic analysis, pH dependency profiles and chemical rescue. This biochemical study, which complements *Ts*XylC crystallographic analysis, allowed to unequivocally identify the two catalytic residues of this retaining β-xylosidase belonging to family GH120.

2. Materials and methods

2.1. Substrates

The substrates 4-NP-β-D-Xyl*p*, 2-nitrophenyl β-D-xylopyranoside (2-NP-β-D-Xyl*p*) and 4-methylumbelliferyl β-D-xylopyranoside (4-MU-β-D-Xyl*p*) were purchased from Sigma. 3,4-dinitrophenyl β-D-xylopyranoside (3,4-dNP-β-D-Xyl*p*) was synthesized in-house as described by Ziser et al. [21].

2.2. Cloning of BaXylB encoding gene

The coding sequence of *Ba*XylB was amplified from the genomic DNA of *B. adolescentis* ATCC15703D-5 using the following primers: forward 5′-AAGTTTGAATACCATGTCAAACCAACCGGC-3′ and reverse 5′-TCAGTTGTTCCATTCCCAAATTCGGATGTG-3′. Using the Gateway technology (Invitrogen), and following the manufacturer instruction, the amplified gene was first cloned into the pCR8/GW/TOPO entry vector and then transferred into the T7 polymerase expression vector pDEST17, downstream of a $(His)_6$ sequence.

2.3. Mutagenesis

Site directed mutagenesis was performed from the pDEST17-*Ba*XylB construct using the Phusion High-Fidelity DNA Polymerase (New England BioLabs) and mutagenic primers designed to include the mutation and, when possible, a restriction site to allow easy identification of the mutation. The mutagenic primers were as follows (the mutated nucleotide are shown in bold within the underlined NNN mutagenic codons and the italic restriction sites): E364X, 5′-ATGGNNNGTCGCTGGCATCAAATT C-3′ (forward, with Gly, G**G**G; Ala, G**C**G; Asp, GA**T**; Gln, **C**AG) and 5′-AGCGACNNNCCA TCCGAAGAATTC-3′ (reverse, with Gly, C**C**C; Ala, C**G**C; Asp, **A**TC; Gln, CT**G**); D393X (*Avr*II), 5′-TGC*TCCCTA*GGCATGTGGATGNNNTG GCAG-3′ (forward, with Gly, G**G**T; Ala, G**C**T; Asn, **A**AT; Gln, GA**A**) and 5′-CTGCCANNNCATCCACATGCC***T****AG****G****GA*GCA-3′ (reverse, with Gly, A**C**C; Ala, A**G**C; Asn, AT**T**; Gln, **T**TC); E416X (*Nco*I), 5′-ATGATT NNNGTGAG***C****CATGG*GCC-3′ (forward, with Gly, G**GC**; Ala, G**C**A; Asp, GA**T**; Gln, **C**AA) and 5′-GGC*CCATG****G****C*TCACNNNAATCAT-3′ (reverse, with Gly, **GC**C; Ala, T**G**C; Asp, **A**TC; Gln, TT**G**). After mutagenesis, samples were treated with *Dpn*I to digest the parental plasmid and then used to transform *Escherichia coli* TOP10 cells. Single colonies were selected and grown overnight in LB supplemented with ampicillin (100 μg/mL), and the plasmids were purified via mini-preparation technique (Qiagen Plasmid Mini kit). The mutated genes were finally sequenced to confirm that only the desired mutations were introduced.

2.4. Overexpression and purification of the N-terminal $(His)_6$-tagged BaXylB wild-type and mutated enzymes

For the production and purification of the N-terminal $(His)_6$-tagged wild-type as well as mutated enzymes, the following procedure was used. A preculture of chemical competent BL21-AI cells transformed with the correct pDEST17-XylB construct was grown overnight in LB supplemented with ampicillin (100 μg/mL) at 37 °C and 140 rpm (orbital diameter: 25 mm). The grown preculture was then diluted to an OD_{600} of 0.01 into 200 mL of ZYM5052 supplemented with ampicillin, 1 mM $CaCl_2$ and 0.02% (w/v) L-arabinose as inductor, and grown at 16 °C and 180 rpm. After 20 h induced cells were harvested, resuspended into binding buffer (20 mM Tris–HCl, pH 7.4, containing 150 mM NaCl and 20 mM imidazole) and disrupted by sonication. The cells extract was then centrifuged to remove cells debris at 10000×*g* for 20 min at 4 °C.

The enzyme was purified by loading the soluble cell extract into a gravity-flow chromatography column packed with 4 mL bed volume of TALON Cobalt affinity resin. Non-specific bound proteins were removed by washing the resin with 4 bed volumes of binding buffer. The bound enzyme was eluted in 10 mL of elution buffer (20 mM Tris–HCl, pH 7.4, containing 150 mM NaCl and 150 mM imidazole). The eluted protein was finally dialyzed against

20 mM sodium phosphate buffer pH 6.0 at 4 °C. Enzyme concentration was determined by measuring the absorbance at 280 nm using a Nanodrop instrument (Wilmington, DE), and using a theoretical extinction coefficient of 141 670 M^{-1} cm^{-1}.

2.5. Determination of hydrolysis stereochemistry by ^1H NMR

Enzyme-mediated hydrolysis of 4-NP-β-D-Xyl*p* was monitored by collecting ^1H NMR using a Bruker Avance II 500.13 MHz spectrometer equipped with a 5 mm-BBI probe and TopSpin 3.0 software, performing reactions in standard 5 mm NMR tube containing 500 µL (final volume) of 5 mM substrate in D_2O. Prior use, 4-NP-β-D-Xyl*p* was freeze-dried from D_2O (99.90%) and the wild-type enzyme was diluted by 10-fold in D_2O, followed by concentration using an Amicon Ultra filter (regenerated cellulose, cutoff 10kDa, Millipore) system; these operations being performed twice. Next, hydrolysis was initiated by the addition of an aliquot of the deuterated enzyme solution (0.05 IU) and reactions were performed at 30 °C. Upon enzyme addition and mixing, the NMR tube was immediately transferred to the spectrometer, and after temperature stabilization, spectra were recorded continuously over 5.52 min during 2 h, thus providing the first spectrum 7.25 min after enzyme addition. Each NMR spectrum was acquired using an excitation flip angle of 90° at a radiofrequency field of 39.4 kHz, and the residual water signal was pre-saturated (65 dB attenuation) during the relaxation delay at a radiofrequency field of 19 Hz. The following acquisition parameters were used: 6 s for the relaxation delay, 32 scans and 4 dummy scans. Before enzyme addition, a ^1H NMR spectrum of the reaction mixture was acquired, serving as the starting point of the reaction. Coupling constants (J) are reported in Hz, chemical shifts (δ) are given in ppm with multiplicity reported as follows: d = doublet. The reference used was the original residual water peak, calibrated at $\delta = 4.71$ ppm at 30 °C [22].

2.6. Kinetic studies

All kinetic studies were carried out by discontinuous assays in glass tubes at 30 °C as follows. Different substrate concentrations were solubilised in 450 µL of 100 mM sodium citrate buffer, pH 5.0, supplemented with 0.1% BSA (w/v). Initial hydrolysis rates were determined by adding 50 µL of properly diluted enzyme to the reaction mix. Enzyme concentrations used for kinetic measurements are mentioned in Table 1. At time intervals, 50 µL of samples were taken and the reaction stopped by the addition of 250 µL of 1 M Na_2CO_3. The released chromogenic groups were determined in micro-plates by reading 200 µL of the stopped reaction mix using a Sunrise spectrophotometer (Tecan). The extinction coefficient used and wavelength monitored for each of the substrate used were: 3,4-dinitrophenol (3,4-dNP), $\Delta\varepsilon = 1.30$ mM^{-1} cm^{-1}, $\lambda = 405$ nm; 4-nitrophenol (4-NP), $\Delta\varepsilon = 1.60$ mM^{-1} cm^{-1}, $\lambda = 405$ nm; 2-nitrophenol (2-NP), $\Delta\varepsilon = 0.31$ mM^{-1} cm^{-1}, $\lambda = 405$ nm; 4-methylumbelliferone (4-MU), $\Delta\varepsilon = 1.68$ mM^{-1} cm^{-1}, $\lambda = 360$ nm. The quantity of released leaving group (LG) was calculated using appropriate standard curves and negative controls containing all of the reactants except the enzyme, in order to remove background noise issued from spontaneous hydrolysis of the substrates. The values of k_{cat} and K_m were determined by non-linear regression analysis using the program SigmaPlot 11.0. In cases where the K_m values were too high to be estimated, k_{cat}/K_m values were calculated from the reaction rates at low substrate concentration. Indeed, when $[S] \ll K_m$ the reaction rates are given by the equation $v = k_{cat}[E]_0[S]/K_m$ and thus k_{cat}/K_m can be calculated by dividing the slope of the plot of $v = f([S])$ by the enzyme concentration.

Table 1
Kinetic parameters of 4-NP-β-D-Xyl*p* hydrolysis by wild-type *Ba*XylB and its Glu^{364}, Asp^{393} and Glu^{416} mutants.

Enzyme	Enzyme concentration (µM)	k_{cat} (s^{-1})	K_m (mM)	k_{cat}/K_m (s^{-1} mM^{-1})
Wild-type	0.01	130.2 ± 8.9	8.4 ± 0.1	15.50
D393A	3.50	<0.001	1.6 ± 1.0	<0.001
D393E	1.14	6.85 ± 1.20	146.2 ± 13.0	0.05
E416G	1.78	0.52 ± 0.02	2.4 ± 0.1	0.22
E416A	6.01	0.15 ± 0.01	2.8 ± 0.1	0.05
E416Q	0.39	6.81 ± 0.21	4.8 ± 0.2	1.42
E416D	0.04	4.20 ± 0.04	1.5 ± 0.1	2.80
E364G	5.81	NS[a]	NS	2.37
E364A	6.25	NS	NS	0.41
E364Q	6.51	NS	NS	0.01
E364D	0.01	407.6 ± 22.4	82.2 ± 7.8	4.96

[a] NS: no saturation.

2.7. pH dependency of k_{cat} and k_{cat}/K_m values

The study of pH dependency of k_{cat} and k_{cat}/K_m values was carried out following the same method used for the kinetic studies, using 4-NP-β-D-Xyl*p* as substrate and the following buffers: 100 mM sodium citrate buffer (pH 4.0–6.0) and 100 mM sodium phosphate buffer (pH 6.0–8.0). The pK_a values assigned to the ionisable groups were determined using the program SigmaPlot 11.0.

2.8. Chemical rescue of the E416A mutant activity

The reaction was performed with 10 mM of 2-NP-β-D-Xyl*p* and 1 M of sodium azide in 100 mM sodium citrate pH 5.0, supplemented with 0.1% BSA (w/v), in presence of 0.24 mg/mL of purified E416A mutant. The reaction medium was then incubated at 30 °C during 2 h. Reaction was stopped by heating the reaction medium at 95 °C for 5 min. The denaturated proteins were removed by filtration with a Centiprep concentrator (cutoff 10kDa, Amicon), centrifuged at 10000×*g* and 4 °C. The reaction medium devoided of enzymes was then analyzed by LC–ELSD, LC–MS and by ^1H NMR after lyophilisation.

2.9. Characterization of the chemical rescue reaction product

LC–ELSD analysis was performed with a Dionex UltiMate 3000 LC System (Thermo scientific) connected to a Varian 380-LC Evaporating Light Scattering Detector (Agilent Technologies). Compounds were separated with a Hypercarb (100 × 4.6) 5 µm column (Thermo Scientific) at 10 °C, using a flow rate of 1 mL/min. Elution was done with water as eluent A and acetonitrile as eluent B, using the following gradient program: 0–10 min, 100:0 (A:B, v/v); 10–20 min, from 100:0 to 50:50; 20 to 30 min, from 50:50 to 20:80; 30 to 35 min, 20:80; from 35 to 40 min, reequilibration at 100:0. Conversions of 2-NP-β-D-Xyl*p* into D-xylose and/or β-D-xylosyl azide (N_3-β-D-Xyl*p*) were monitored with the ELSD detector set-up with the following parameters: evaporation 70 °C, nebulisation 40 °C and nitrogen flow 1 slm. Retention times for β-D-Xyl*p*, α-D-Xyl*p*, N_3-β-D-Xyl*p* and 2-NP-β-D-Xyl*p* were 2.4, 3.1, 14.3 and 23.3 min, respectively. LC–MS analysis was performed with a Dionex UltiMate 3000 LC System (Thermo scientific) but connected to a MSQ Plus mass spectrometer (Thermo scientific). The compounds were separated with the same column and method as described above and analyzed with the MS instrument operated in an electrospray negative ionization mode (ESI^-) at 30 V and 500 °C, and scanned from 100 to 1500 ms.

^1H NMR spectra of the reaction mixture and standards were recorded at 298 K in CD_3OD, calibrated to the residual solvent signal [22]. Mass spectrometry analyses of the crude reaction mixture were also performed in positive and negative ionization mode (ESI)

with a Bruker Daltonics Esquire 3000 + mass spectrometer (PCN-ICMG, Grenoble) and revealed mass of 198 and 217 corresponding to $[M+Na]^+$ and $[M+N_3]^-$ D-xylopyranosyl azide adducts, respectively.

3. Results and discussion

3.1. Stereochemical outcome of the BaXylB-catalyzed hydrolysis and its mode of action

Members of the GH120 family have been proposed to be retaining glycosidases, which achieve glycosidic bond hydrolysis via the canonical two-step double-displacement mechanism, through the involvement of two carboxylic amino acids [19]. As illustrated in Scheme 1, during the first step of this general mechanism, called the glycosylation step, one of these two carboxylic residues, the nucleophile, attacks the substrate anomeric carbon forming a covalent glycosyl-enzyme intermediate. Concomitantly, the second carboxylic residue, the acid/base catalyst, acts as a general acid, protonating the interglycosidic oxygen, and thereby assisting and stabilizing the LG departure. In the second step instead, called the deglycosylation step, the acid/base catalyst acts as a general base, activating a water molecule which in turn attacks the glycosyl-enzyme intermediate at its anomeric center, to release the newly formed reducing end with retention of the anomeric configuration.

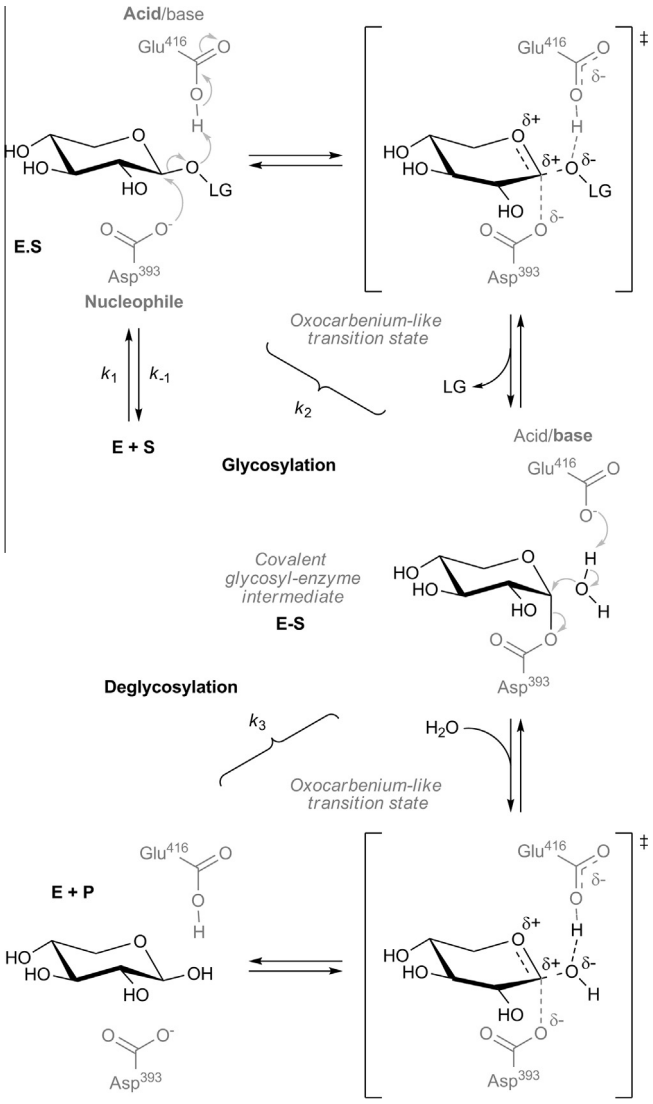

Scheme 1. Two-step displacement mechanism of retaining GHs (*Ba*XylB numbering), showing the glycosylation and deglycosylation steps, and transition states. The leaving group (LG) can be either a chromogenic compound (e.g. 4-NP), glycoside (e.g. XOS) or carbohydrate monomer. The kinetic constants correspond to the following equations: $k_{cat} = k_2k_3/(k_2 + k_3)$, $K_m = (k_{-1} + k_2)k_3/(k_2 + k_3)k_1$ and $k_{cat}/K_m = k_1k_2/(k_{-1} + k_2)$.

The stereochemical course of the *Ba*XylB-catalyzed hydrolytic reaction was monitored by ^{1}H NMR spectroscopy (Fig. 1). Prior to the addition of the enzyme, the spectrum of the anomeric proton region (4.5–5.3 ppm) displayed a doublet centered at 5.23 ppm (7.4 Hz), corresponding to the signal of the axial *H*-1 protons of 4-NP-β-D-Xyl*p*, but no signal corresponding to D-xylose was detectable. Immediately (i.e. within the first 15 min after the addition of the enzyme), a new doublet was observed at 4.57 ppm with a splitting of 7.9 Hz, corresponding to the axial *H*-1 of the reducing β-D-Xyl*p*. The equatorial *H*-1 of α-D-Xyl*p* counterpart (5.18 ppm, d, 3.7 Hz) appeared later as a result of mutarotation. This spectroscopic analysis unequivocally demonstrates that GH120 *Ba*XylB catalyzes hydrolysis with retention of the anomeric configuration and proceeds via a two-steps displacement mechanism (Scheme 1), being consistent with that proposed for enzymes of the GH120 family [19].

3.2. Identification of the key acidic residues by site directed mutagenesis

From the protein sequence alignment of *Ba*XylB with *Ts*XylC, which shares 48% of sequence identity [17], and the inspection of *Ts*XylC protein structure co-crystallized with D-xylose (PDB number: 3VSV) and xylobiose (PDB number: 3VSU) it was possible to list all the equivalent *Ba*XylB residues forming the active site.

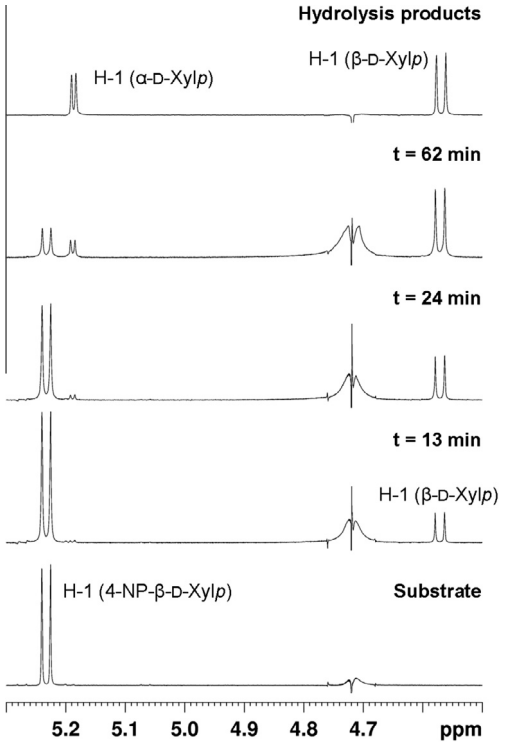

Fig. 1. Time course of 4-NP-β-D-Xyl*p* hydrolysis by *Ba*XylB. ^{1}H NMR spectra, in D_2O at 303 K, of the anomeric region of the substrate (i.e. before addition of enzyme), after 13, 24, and 62 min of incubation with the enzyme, and hydrolysis products (as a result of mutarotation).

Among them only three residues bear a carboxyl group, Glu^{364}, Asp^{393} and Glu^{416}, which correspond to the Glu^{353}, Asp^{382} and Glu^{405} residues (Fig. 2) that were identified in the active site of *Ts*XylC [20].

In order to identify which among these three putative catalytic residues plays the role either of the nucleophile or the acid/base catalyst, an extensive study was performed, by mutating these three residues into glycine, alanine, asparagine or glutamine and thus by determining the kinetic parameters of these mutants using 4-NP-β-D-Xyl*p* as substrate (Table 1). Asp^{393} mutation displays the most dramatic effect on *Ba*XylB activity, since k_{cat} value for D393A was severely reduced of about 10^5-fold compared to the wild-type enzyme. As expected, activity was partially restored by replacing Asp^{393} by glutamate, while the K_m value increased by 17-fold. As already reported for retaining GHs, the mutation of the nucleophile catalyst usually has the greater impact on enzyme activity, sometimes completely abolishing it [23,24]. The magnitude of activity decrease obtained by Asp^{393} mutation, which is comparable to that observed for other retaining GHs [23,25], indicates that Asp^{393} would play the role of nucleophile. Mutations of Glu^{416} also affect activity, but to a less extent. For Glu^{416} mutants, k_{cat} were 19 to 868-fold lower than that of the wild-type, while K_m values were not significantly affected by these mutations. Additionally, mutation of Glu^{364} also affected enzyme activity, but in a different way, since it was difficult to obtain reliable kinetic constants. Indeed, at the highest substrate concentration used (70 mM), the activities determined were still at the initial increasing part of the Michaelis–Menten curve, which suggest very high K_m values for these mutants. However, for mutant E364Q, it was possible to determine the k_{cat} and K_m values, which are 4- and 25-fold higher than the wild-type ones, respectively. Because of this great K_m increase when mutated, Glu^{364} was thought to be involved in substrate binding, as proposed for *Ts*XylC [20].

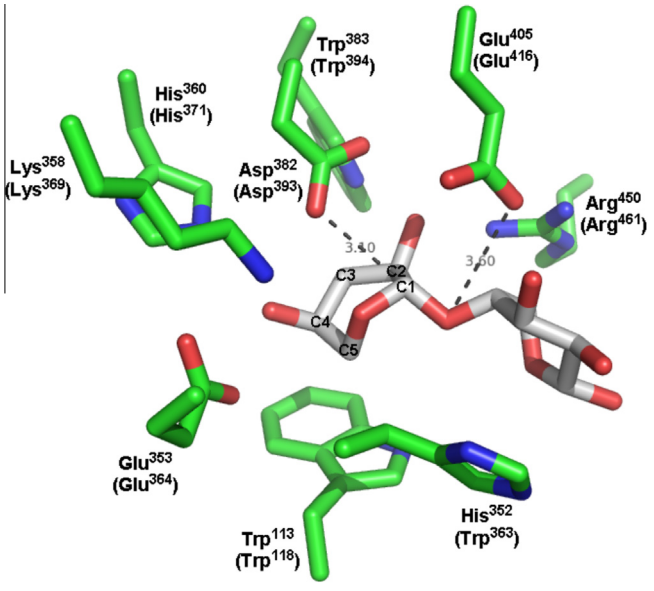

Fig. 2. Residues surrounding xylobiose in the active site of the GH120 *Ts*XylC (PDB accession number: 3VSU) [20]. The corresponding amino acids in *Ba*XylB are mentioned in parentheses. Interatomic distances are labeled in Å. Among the three carboxylic residues within the active site structure of the Michaelis *Ts*XylC-xylobiose complex, Glu^{353} is too far (more than 5.4 Å) from both the anomeric carbon and the glycosidic oxygen to be a catalytic residue. Asp^{382} is properly positioned (at 3.1 Å) for a nucleophilic attack to the anomeric carbon of the distorted non-reducing D-Xyl*p* unit, displaying a quasi-axial orientation for the scissile glycosidic bond. The positioning of Glu^{405} is somehow ambiguous. Although well located to serve as the general acid/base catalyst, it appears slightly too far (3.6 Å) from the glycosidic oxygen for proton donation [32,33]. This is probably due to the incorrect positioning of the reducing D-Xyl*p* unit, as a consequence of an unclear electron density map.

3.3. Kinetic analysis of wild-type and Glu^{416} mutants with substrates bearing different leaving groups

As in retaining glycosidases the acid/base catalyst has a double role in catalysis, its substitution with non-acidic amino-acids should affects the rates of both reaction steps, even though the effect on each step will be different. The analysis of the kinetic properties of such mutants with substrate bearing different LGs is a common strategy for studying the mechanistic action of glycosidases. Indeed, in the first step, the effect of the mutation strongly depends on the leaving ability of the aglycone group. Thus, the glycosylation rates of substrates with poor LGs ($pK_a > 8$), which need protonic assistance by the catalytic acid/base residue, are more strongly affected compared to those obtained with substrates bearing good LGs. In the deglycosylation step instead, as the covalent glycosyl-enzyme intermediate is the same, the effect on the hydrolytic rates might be unaffected for all substrates. If the glycosylation step is rate-limiting, a correlation between pK_a of the aglycone group and k_{cat} should be observed. If instead the deglycosylation step is rate limiting, k_{cat} will be invariant with substrate reactivity [26].

In order to gain more information on the mechanistic role played by the Glu^{416} residue, kinetic constants of the E416A, E416G, E416Q and E416D mutants were determined using substrates bearing different LGs and compared to those obtained for the wild-type. Kinetic constants (Table 2), as well as Brønsted plots (Fig. 3) show that the wild-type k_{cat} and K_m values are similar for all the tested substrates (with $pK_a < 8$, i.e. bearing good LG) indicating that here deglycosylation is the rate-limiting step. On the contrary, k_{cat} values measured for the Glu^{416} mutants were reduced with all the tested substrates. Moreover, k_{cat} values decreased with pK_a increase, suggesting that (i) with a substrate bearing a good LG like 3,4-dNP-β-D-Xyl*p* ($pK_a = 5.36$), the deglycosylation step still is the rate-limiting step, as for the wild-type, and (ii) with substrates bearing 'poorer' but still good LGs, the glycosylation step becomes at least partially rate-limiting. This is exactly one of the effects expected for an enzyme incapable of proton assistance because devoided of the general acid/base catalytic residue. Moreover, the

Table 2
Kinetic parameters of aryl β-D-xyloside hydrolysis by wild-type *Ba*XylB and its Glu^{416} mutants.

Aglycone	pK_a[a]	Enzyme	k_{cat} (s^{-1})	K_m (mM)	k_{cat}/K_m (s^{-1} mM^{-1})
3,4-dNP	5.36	Wild-type	114.07	3.4	33.55
		E416G	22.23	1.3	17.10
		E416A	4.42	1.8	2.46
		E416Q	16.81	1.6	10.50
		E416D	18.45	1.8	10.25
4-NP	7.18	Wild-type	130.19	8.4	15.50
		E416G	0.52	2.4	0.22
		E416A	0.15	2.8	0.05
		E416Q	6.81	4.8	1.42
		E416D	4.20	1.5	2.80
2-NP	7.22	Wild-type	166.59	3.8	43.84
		E416G	7.88	0.60	13.05
		E416A	3.41	0.40	8.56
		E416Q	25.00	0.79	31.29
		E416D	37.54	0.75	50.32
4-MU	7.53	Wild-type	134.01	1.6	83.76
		E416G	0.01	0.10	0.06
		E416A	0.003	0.39	0.008
		E416Q	0.29	0.25	1.19
		E416D	1.95	0.20	9.78

[a] pK_a values from [29,34].

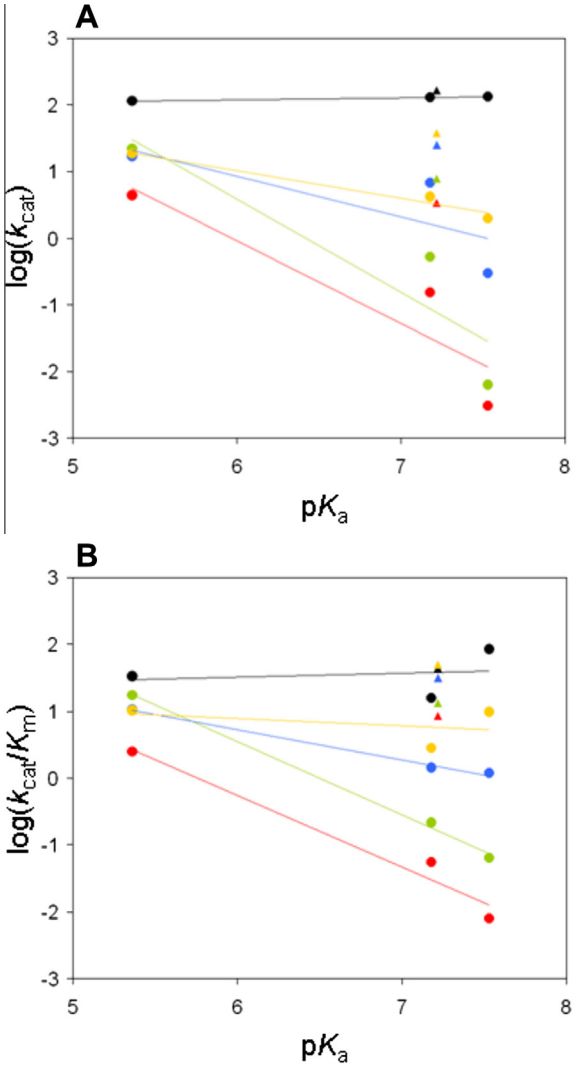

Fig. 3. Brønsted plots of aryl β-D-xyloside hydrolysis by wild-type *Ba*XylB (black) and its E416A (red), E416G (green), E416Q (blue) and E416D (orange) mutants. (A) plot of log(k_{cat}) versus pK_a of the aglycone group and (B) plot of log(k_{cat}/K_m) versus pK_a of the aglycone group. The values obtained from 2NP-β-D-Xyl*p* (▲) have been excluded from linear fitting.

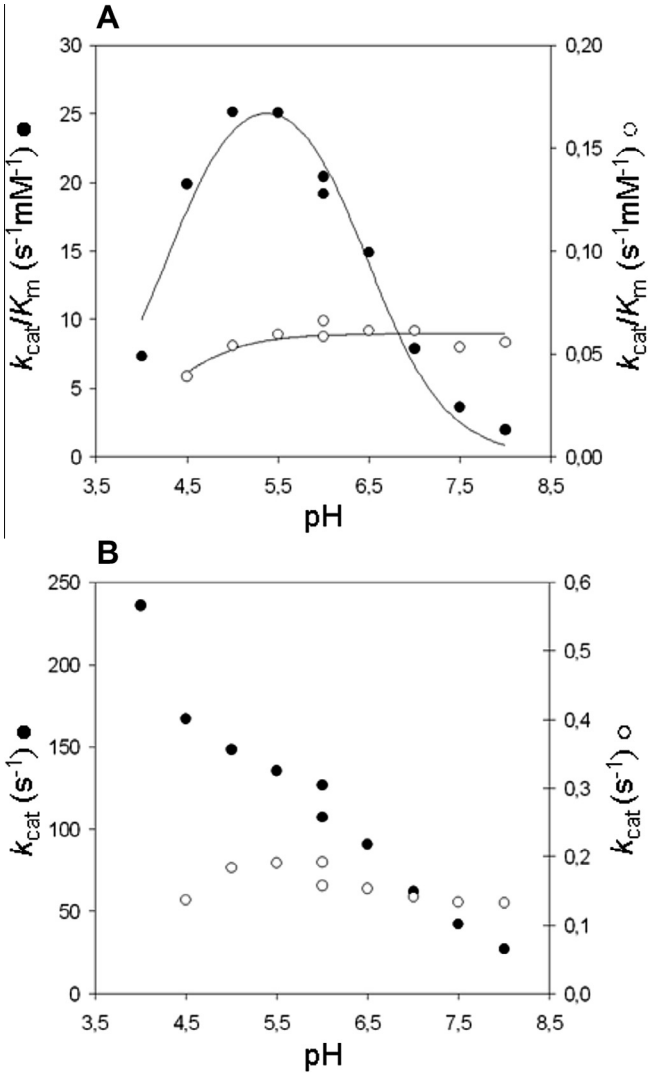

Fig. 4. pH dependency of k_{cat}/K_m (A) and k_{cat} (B) for hydrolysis of 4-NP-β-D-Xyl*p* by the wild-type *Ba*XylB (●) and its E416A mutant (○).

high negative Brønsted coefficient β_{lg} of −1.3 and −1.2, measured for the E416G and E416A mutants respectively, indicates high amounts of negative charges on the glycosidic oxygen in the transition state (i.e. significant cleavage of the interglycosidic bond in the TS), consistent with relatively little proton donation to the forming phenolate anion caused by the impaired proton assistance of this acid/base mutants.

By plotting the log(k_{cat}/K_m) as function of pK_a, Brønsted coefficients of −1.1 (for E416G and E416A) were obtained for the glycosylation step, values similar to that obtained by plotting the log (k_{cat}) – which instead reflects both the glycosylation and deglycosylations steps – versus pK_a, thus suggesting that the same event was mainly monitored.

The change of the reaction rate-limiting step for the Glu^{416} mutants, highlighted by the strong correlation between their k_{cat} and substrate pK_a, strongly supports for Glu^{416} as the acid/base catalyst.

An exception of this general trend was observed with 2-NP-β-D-Xyl*p*, for which k_{cat} values similar to the most reactive substrate 3,4-dNP-β-D-Xyl*p* were obtained. This suggests that for 2-NP-β-D-Xyl*p* the deglycosylation step seems the slowest step. Furthermore, k_{cat}/K_m obtained with 2-NP-β-D-Xyl*p* was higher than that obtained with 3,4-dNP-β-D-Xyl*p*, also due to an higher impact on the K_m values for the former substrate. This suggests that with 2-NP-β-D-Xyl*p* the first step is faster and, as a consequence, would led to the accumulation of a higher amount of glycosyl-enzyme intermediate, resulting in a lower K_m value. This was surprising, since according to its pK_a (7.22), the leaving ability of 2-NP should be lower than that of 3,4-dNP (pK_a = 5.36). Thereby, we can speculate that in the *orto* position of the phenyl ring, the nitro group would either specifically interact with residues of the catalytic site, modifying the overall binding mode of the substrate or taking advantage of hydrophobic packing, towards by stabilizing the TS of the glycosylation step.

3.4. pH dependency of the wild-type and E416A catalytic constants

The pH dependency profile of kinetic parameters is another way to investigate the role of specific residues in catalysis. While the plot of k_{cat} versus pH reflects the pK_a values of ionisable groups in the enzyme-substrate complex, that of k_{cat}/K_m as a function of pH reflects the pK_a values of the free enzyme. Both for the wild-type *Ba*XylB and its E416A mutant, the values of k_{cat} and k_{cat}/K_m were measured in the pH range of 4.0–8.0, using 4-NP-β-D-Xyl*p*

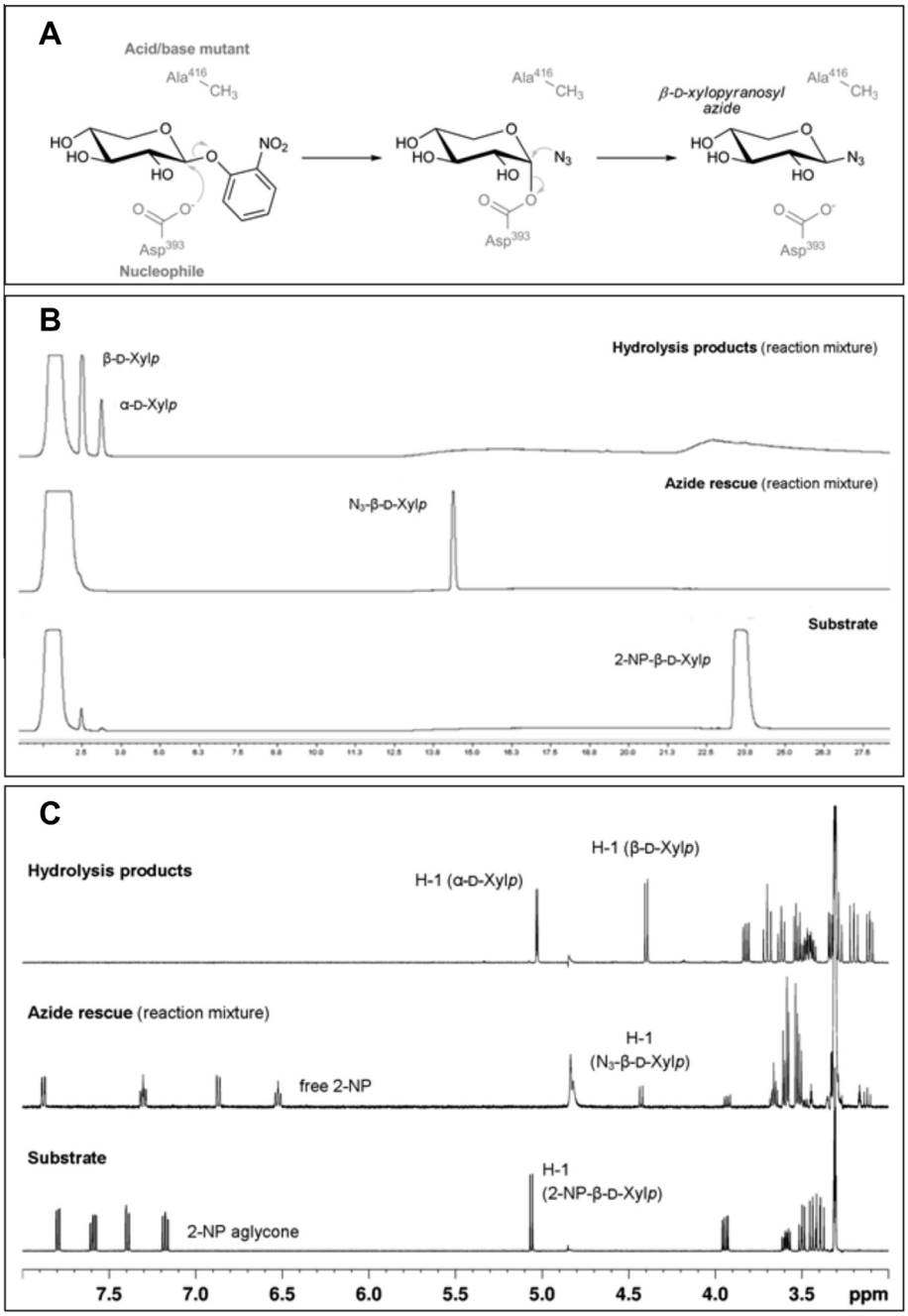

Fig. 5. Formation of the β-D-xylopyranosyl azide product obtained by the E416A *Ba*XylB mutant. (A) Schematic representation for activity rescue by azide. (B) LC–ELSD analysis of the reaction products obtained after 1 h of incubation from 2-NP-β-D-Xyl*p* hydrolysis in absence and in additional presence of 1 M sodium azide. (C) ^{1}H NMR spectra, at 298 K in CD_3OD, of the reaction mixture obtained from 2-NP-β-D-Xyl*p* hydrolysis in the presence of 1 M sodium azide and controls (substrate and hydrolysis products, i.e. anomeric mixture of D-Xyl*p*) thereof.

as substrate (Fig. 4). The pH dependency profile of the wild-type k_{cat}/K_m values is a bell-shape curve typical of glycosidases. pK_a values of 4.3 and 6.5 reflects the ionization state of the two carboxylic catalytic residues in the active site, acid pK_a being assigned to the nucleophile, and basic one to the acid/base catalyst. A pK_a of 6.5 is high for a carboxylic residue, but similar values have been observed for other glycosidases [23,27,28]. The pH dependency profile of k_{cat} values, in the tested pH range was different. A single ionization curve was obtained, with only a basic limb, from which an apparent pK_a of 6.5 was calculated, since no saturation of k_{cat} values was observed at the lowest tested pH. Such differences of pH dependency profiles between the free enzyme and the substrate-enzyme complex has also already been observed for a GH1 retaining β-glucosidase from an *Agrobacterium* sp. [29]. Unfortunately, measurements of k_{cat} at pH values lower than 4.0 were precluded due to enzyme instability. This hampered us to know if the pK_a assigned to the nucleophile would have been shifted to a lower value, or if after the formation of the enzyme-substrate complex, the nucleophile would not be protonated anymore, due to drastic change in the proton exchange 'cycle'.

In contrast with what was observed with the wild-type, the pH dependency of E416A activity was overall drastically reduced especially at high pH values, either for the free enzyme or for its complexed form, suggesting that the acid/base catalyst has been removed. For both the free and complexed forms of E416A mutants, the acid limb pK_a is 4.3, suggesting that in this case the

introduction of the mutation may have created sufficient space between the catalytic site and the surface of the enzyme to permit proton exchange with the reaction medium.

3.5. Chemical rescue of the E416A mutant

The use of external nucleophilic anions such as azide has been shown to enhance the rate of enzymes devoided of their catalytic residues. Indeed, the replacement of the nucleophile or the acid/base catalyst with smaller residues, such as glycine or alanine, is generally sufficient to create a cavity in which exogeneous small nucleophile compounds can penetrate and attack the anomeric center of the substrate or the covalent glycosyl-enzyme intermediate, depending on the catalytic residue replaced, to form a glycosyl azide product. Since the products of these reactions are stereospecific α- or β-glycosyl azides, this strategy allows not only identification of the catalytic residues but also to determine if the mutated residue is the nucleophile or the general acid/base catalyst (Fig. 5A). Using 2-NP-β-D-Xyl*p* as substrate, a 16-fold hydrolysis rate increase was obtained for the E416A mutant, in the presence of 1 M azide. This chemical rescue was not as significant as previously reported for other glycosidases, for which rate increase up to 10^2–10^3-fold were obtained [23,30,31]. Nevertheless, LC–ELSD analysis of the reaction product revealed the formation of a new single product in the presence of azide, instead of D-xylose (Fig. 5B). Reaction product characterization by LC–MS analysis revealed, for this newly-formed sole peak, a mass of 217 corresponding to $[M+N_3]^-$ D-xylopyranosyl azide adduct. Furthermore, the reaction mixture containing the D-xylopyranosyl azide was analyzed by ^{1}H NMR (Fig. 5C). The complete disappearance of the *H*-1 signal of 2-NP-β-D-Xyl*p* at 5.06 ppm (d, 7.1 Hz) was accompanied by parallel changes of the 2-NP aglycone signals into free 2-NP signals (signals between 6.5 and 7.9 ppm) and the appearance of one alone new anomeric signal at 4.43 ppm (d, 8.5 Hz) attributed to the *H*-1 of the β-D-xylopyranosyl azide (N_3-β-D-Xyl*p*) [23].

All together these data, including the kinetic behavior displayed by the Glu^{416} mutants as well as the pH dependency of E416A activity and its chemical rescue, provide definitive evidence that this GH120 β-xylosidase uses a retaining mechanism of glycoside hydrolysis, with Glu^{416} (*Ba*XylB numbering) playing the role of the acid/base catalyst and Asp^{393} that of the nucleophile, assisted by Glu^{364} to stabilize the enzyme-substrate covalent intermediate.

Acknowledgements

This work was funded by the Institut National de la Recherche Agronomique (INRA). We thank Nelly Monties for technical assistance on LC–ELSD and LC–MS equipments provided by the ICEO facility dedicated to enzyme screening and discovery, part of the Integrated Screening Platform of Toulouse (PICT, IBiSA). We cordially thank David Guieysse and Alvaro Lafraya for their helpful expertise in LC–MS. MetaToul (Metabolomics & Fluxomics Facilities, Toulouse, France, www.metatoul.fr) and its staff members (Lindsay Peyriga, Edern Cahoreau and Jean-Charles Portais) are gratefully acknowledged for the technical support and access to NMR facility. MetaToul is part of the national infrastructure MetaboHUB-ANR-11-INBS-0010 (The French National infrastructure for metabolomics and fluxomics, www.metabohub.fr). MetaToul is supported by grants from the Région Midi-Pyrénées, the European Regional Development Fund, the SICOVAL, the Infrastructures en Biologie Sante et Agronomie (IBiSa, France), the Centre National de la Recherche Scientifique (CNRS) and INRA. The authors also acknowledge support from the Mass spectrometry facility of the Chemistry Nanobio Platform-ICMG (FR 2607), Grenoble.

References

[1] Turnbaugh, P.J., Hamady, M., Yatsunenko, T., Cantarel, B.L., Duncan, A., Ley, R. E., Sogin, M.L., Jones, W.J., Roe, B.A., Affourtit, J.P., Egholm, M., Henrissat, B., Heath, A.C., Knight, R. and Gordon, J.I. (2009) A core gut microbiome in obese and lean twins. Nature 457, 480–484.

[2] Qin, J., Li, Y., Cai, Z., Li, S., Zhu, J., Zhang, F., Liang, S., Zhang, W., Guan, Y., Shen, D., Peng, Y., Zhang, D., Jie, Z., Wu, W., Qin, Y., Xue, W., Li, J., Han, L., Lu, D., Wu, P., Dai, Y., Sun, X., Li, Z., Tang, A., Zhong, S., Li, X., Chen, W., Xu, R., Wang, M., Feng, Q., Gong, M., Yu, J., Zhang, Y., Zhang, M., Hansen, T., Sanchez, G., Raes, J., Falony, G., Okuda, S., Almeida, M., LeChatelier, E., Renault, P., Pons, N., Batto, J. M., Zhang, Z., Chen, H., Yang, R., Zheng, W., Li, S., Yang, H., Wang, J., Ehrlich, S. D., Nielsen, R., Pederson, O., Kristiansen, K. and Wang, J. (2012) A metagenome-wide association study of gut microbiota in type 2 diabetes. Nature 490, 55–60.

[3] Karlsson, F.H., Tremaroli, V., Nookaew, I., Bergström, G., Behre, C.J., Fagerberg, B., Nielsen, J. and Bäckhed, F. (2013) Gut metagenome in European women with normal, impaired and diabetic glucose control. Nature 498, 99–103.

[4] Karlsson, F.H., Fåk, F., Nookaew, I., Tremaroli, V., Fagerberg, B., Petranovic, D., Bäckhed, F. and Nielsen, J. (2012) Symptomatic atherosclerosis is associated with an alterated gut metagenome. Nat. Commun. 3, 1245.

[5] Hidaka, H., Tashiro, Y. and Eida, T. (1991) Proliferation of bifidobacteria by oligosaccharides and their useful effect on human health. Bifidobact. Microflora 10, 65–79.

[6] Hsu, C.K., Liao, J.W., Chung, Y.C., Hsieh, C.P. and Chan, Y.C. (2004) Xylooligosaccharides and fructooligosaccharides affect the intestinal microbiota and precancerous colonic lesion development in rats. J. Nutr. 134, 1523–1528.

[7] Campbell, J.M., Fahey, J. and Wolf, B.W. (1997) Selected indigestible oligosaccharides affect large bowel mass, cecal and fecal short-chain fatty acids, pH and microflora in rats. J. Nutr. 127, 130–136.

[8] Ebringerova, A., Hromadkova, Z., Alfodi, J. and Hribalova, V. (1998) The immunologically active xylan from ultrasound-treated corncobs: extractability, structure and properties. Carbohydr. Polym. 37, 231–239.

[9] Ebringerova, A., Kardosova, A., Hromadkova, Z., Malovikova, A. and Hribalova, V. (2002) Immunomodulatory activity of acidic xylans in relation to their structural and molecular properties. Int. J. Biol. Macromol. 30, 1–6.

[10] Santos, A., San Mauro, M. and Diaz, D.M. (2006) Prebiotics and their longterm influence on the microbial populations of the mouse bowel. Food Microbiol. 23, 498–503.

[11] Gibson, G.R., Cummings, J.H. and McFarlane, G.T. (1991) Growth and activities of sulphate-reducing bacteria in gut contents of healthy subjects and patients with ulcerative colitis. FEMS Microbiol. Ecol. 86, 103–112.

[12] Babidge, W., Millard, S. and Roediger, W. (1998) Sulfides impair short chain fatty acid beta-oxidation at acyl-CoA dehydrogenase level in colonocytes: implications for ulcerative colitis. Mol. Cell. Biochem. 181, 117–124.

[13] Pitcher, M.C.L. and Cummings, J.H. (1996) Hydrogen sulphide: a bacterial toxin in ulcerative colitis? Gut 39, 1–4.

[14] Loubinoux, J., Bronowicki, J.P., Pereira, I.A.C., Mougenel, J.L. and Le Faou, A.E. (2002) Sulfate-reducing bacteria in human feces and their association with inflammatory bowel diseases. FEMS Microbiol. Ecol. 40, 107–112.

[15] Lombard, V., Golaconda Ramulu, H., Drula, E., Coutinho, P.M. and Henrissat, B. (2014) The carbohydrate-active enzymes database (CAZy) in 2013. Nucleic Acids Res. 42, D490–D495.

[16] Cecchini, A.D., Laville, E., Laguerre, S., Robe, P., Leclerc, M., Doré, J., Henrissat, B., Remaud-Siméon, M., Monsan, P. and Potocki-Véronèse, G. (2013) Functional metagenomic reveals novel pathways of prebiotic break down by human gut bacteria. PLoS One 8, e72766.

[17] Lagaert, S., Pollet, A., Delcour, A.J., Lavigne, R., Courtin, M.C. and Volckaert, G. (2011) Characterization of two β-xylosidases from *Bifidobacterium adolescentis* and their contribution to the hydrolysis of prebiotic xylooligosaccharides. Appl. Microbiol. Biotechnol. 92, 1179–1185.

[18] Lagaert, S., Van Campenhout, S., Pollet, A., Bourgois, T.M., Delcour, J.A., Courtin, C.M. and Volckaert, G. (2007) Recombinant expression and characterization of a reducing-end xylose-releasing exo-oligoxylanase from *Bifidobacterium adolescentis*. Appl. Environ. Microbiol. 73, 5374–5377.

[19] Shao, W., Xue, Y., Wu, A., Kataeva, I., Pei, J., Wu, H. and Wiegel, J. (2011) Characterization of a novel β-xylosidase, XylC, from *Thermoanaerobacterium saccharolyticum* JW/SL-YS485. Appl. Environ. Microbiol. 77, 719–726.

[20] Huang, C.H., Sun, Y., Ko, T.P., Chen, C.C., Zheng, Y., Chan, H.C., Pang, X., Wiegel, J., Shao, W. and Guo, R.T. (2012) The substrate/product binding modes of a novel GH120 β-xylosidase (XylC) from *Thermoanaerobacterium saccharolyticum* JW/SL-YS485. Biochem. J. 448, 401–407.

[21] Ziser, L., Setyawati, I. and Withers, S.G. (1995) Syntheses and testing of substrates and mechanism-based inactivators for xylanases. Carbohydr. Res. 274, 137–153.

[22] Gottlieb, H.E., Kotlyar, V. and Nudelman, A. (1997) NMR chemical shifts of common laboratory solvents as trace impurities. J. Org. Chem. 62, 7512–7515.

[23] Bravman, T., Belakhov, V., Solomon, D., Shoham, G., Henrissat, B., Baasov, T. and Shoham, Y. (2003) Identification of the catalytic residues in family 52 glycoside hydrolase, a β-xylosidase from *Geobacillus stearothermophilus* T-6. J. Biol. Chem. 278, 26742–26749.

[24] MacLeod, A.M., Tull, D., Rupitz, K., Warren, A.J. and Withers, S.G. (1996) Mechanistic consequences of mutation of active site carboxylates in a retaining β-1,4-glycanase from *Cellulomonas fimi*. Biochemistry 35, 13165–13172.

[25] Ly, H.D. and Withers, S.G. (1999) Mutagenesis of glycosidases. Annu. Rev. Biochem. 68, 487–522.
[26] Zechel, L.D. and Withers, S.G. (2000) Glycosidase mechanisms: anatomy of a finely tuned catalyst. Acc. Chem. Res. 33, 11–18.
[27] Shallom, D., Belakhov, V., Solomon, D., Gilead-Gropper, S., Baasov, T., Shoham, G. and Shoham, Y. (2002) The identification of the acid-base catalyst of α-arabinofuranosidase from *Geobacillus stearothermophilus* T-6, a family 51 glycoside hydrolase. FEBS Lett. 514, 163–167.
[28] Vocadlo, J.D., Wicki, J., Rupitz, K. and Withers, S.G. (2002) Mechanism of *Thermoanaerobacterium saccharolyticum* β-xylosidase: kinetic studies. Biochemistry 41, 9727–9735.
[29] Kempton, J.B. and Whiters, S.G. (1992) Mechanism of *Agrobacterium* β-glucosidase: kinetic studies. Biochemistry 31, 9961–9969.
[30] Wang, Q., Trimbur, D., Graham, R., Warren, R.A.J. and Withers, S.G. (1995) Identification of the acid/base catalyst in *Agrobacterium faecalis* β-glucosidase by kinetic analysis of mutants. Biochemistry 34, 14554–14562.
[31] MacLeod, A.M., Lindhorst, T., Withers, S.G. and Warren, R.A.J. (1994) The acid/base catalyst in the exoglucanase/xylanase from *Cellulomonas fimi* is glutamic acid 127: evidence from detailed kinetic studies of mutants. Biochemistry 33, 6371–6376.
[32] Heightman, T.D. and Vasella, A.T. (1999) Recent insights into inhibition, structure, and mechanism of configuration-retaining glycosidases. Angew. Chem. Int. Ed. 38, 750–770.
[33] Nerinckx, W., Desmet, T., Piens, K. and Claeyssens, M. (2005) An elaboration on the *syn-anti* proton donor concept of glycoside hydrolases: electrostatic stabilisation of the transition state as a general strategy. FEBS Lett. 579, 302–312.
[34] Sinnott, L.M. and Souchard, J.L.I. (1973) Effect of aglycone nature and α-deuterium substitution on the hydrolysis of aryl galactosides. Biochem. J. 133, 89–98.